COLO – HEP – 343
June 1994

B PHYSICS AT THRESHOLD:

RECENT RESULTS FROM ARGUS AND CLEO II

James G. Smith
Physics Department, University of Colorado
Boulder, Colorado 80309-0390

ABSTRACT

Recent results from CLEO and ARGUS for a variety of B decays are presented. Results from two-body $b \to c$ transitions address the factorization hypothesis. Semileptonic $b \to c$ and $b \to u$ transitions are studied and values for V_{cb} and V_{ub} are extracted. ARGUS has events which are consistent with an inclusive $b \to s$ gluon signal, permitting a branching fraction to be extracted. CLEO is becoming sensitive to a variety of rare B decays. The penguin decay $B \to K^*\gamma$ has been observed by CLEO and a significant signal has also been measured in the sum of the modes $B^0 \to K^+\pi^-$ and $B^0 \to \pi^+\pi^-$.

Invited talk presented at *Les Rencontres de Physique*
La Thuile, Italy, March 6-12, 1994

---

* This work was supported by the U. S. Department of Energy under grant number DE-FG02-91ER40672

I. Introduction

The latest results from ARGUS and CLEO II are probing fundamental aspects of the standard model with improved precision. Of particular interest are the measurements providing information on the elements of the CKM quark-mixing matrix[1]:

$$\begin{pmatrix} V_{ud} & V_{us} & V_{ub} \\ V_{cd} & V_{cs} & V_{cb} \\ V_{td} & V_{ts} & V_{tb} \end{pmatrix} \tag{I.1}$$

Results from semileptonic $b \to c$ transitions determine the element V_{cb}; semileptonic $b \to u$ transitions and the decay $B^0 \to \pi^+\pi^-$ determine the element V_{ub}; the inclusive electromagnetic "penguin" decay $b \to s\gamma$ and the exclusive decay $B \to K^*\gamma$ provide information on V_{ts}; and eventually measurements of the decays $B \to \rho\gamma$ and $B \to \omega\gamma$ will provide information on V_{td}.

II. Hadronic B decays and factorization

Calculations by Bauer, Stech and Wirbel[2] (BSW) describe hadronic heavy-meson decays by using factorization and a phenomenological approach. These have been used with some success for the past seven years. There are two amplitudes, a_1 and a_2, corresponding to the external spectator and internal spectator (color-suppressed) diagrams, respectively. These amplitudes can be related to coefficients in the QCD Hamiltonian,

$$a_1 \sim C_1 + \xi C_2 \qquad a_2 \sim C_2 + \xi C_1, \tag{II.1}$$

where $\xi = 1/N_C$, with N_C the number of colors, and the coefficients C_1 and C_2 evaluated at the QCD mass scale $\mu = m_c$ or $\mu = m_b$. However, a_1 and a_2 cannot yet be calculated reliably and are generally taken to be constants to be determined by experiment. Once determined, they can be used to predict decay rates for all two-body hadronic B decays. With the advent of heavy-quark effective theory (HQET),[3] improvements to this approach are possible.[4] A recent calculation[5] has used the BSW general approach together with recent experimental input and HQET to derive improved rate predictions, though uncertainties are still large.

In order to determine the amplitudes a_1 and a_2, measured branching fractions are compared with the predictions of the models discussed above. The CLEO

II collaboration uses the color-suppressed decays $B \to \psi K$ and $B \to \psi K^*$ to determine[6)]

$$|a_2| = 0.26 \pm 0.01 \pm 0.01 \pm 0.02, \tag{II.2}$$

where the last error is due to uncertainty in the relative amount of B^- and B^0 production and the lifetimes of each. In order to determine a_1, CLEO has used the decays $\bar{B}^0 \to D^+\pi^-$, $D^+\rho^-$, $D^{*+}\pi^-$ and $D^{*+}\rho^-$. The invariant-mass distributions for these decays, along with the analogous decays of the B^-, are shown in Figs. 1 and 2. By fitting to the branching fractions for these four decays (given in Table 1)[7)], they find

$$|a_1| = 1.15 \pm 0.04 \pm 0.05 \pm 0.09. \tag{II.3}$$

TABLE 1. Measured branching fractions for four B^0 decay modes.

$\bar{B}^0$ Mode	D mode	# of events	$\mathcal{B}(\%)$	$\mathcal{B}$ average (%)
$D^+\pi^-$	$K^-\pi^+\pi^+$	80.6±9.8	0.29±0.04	0.29±0.04±0.03 ± 0.05
$D^+\rho^-$	$K^-\pi^+\pi^+$	78.9±10.7	0.81±0.11	0.81±0.11±0.12 ± 0.13
$D^{*+}\pi^-$	$K^-\pi^+$	19.4±4.5	0.22±0.05	0.26±0.03±0.04 ± 0.01
	$K^-\pi^+\pi^0$	31.9±6.4	0.30±0.06	
	$K^-\pi^+\pi^+\pi^-$	20.5±5.2.	0.27±0.07	
$D^{*+}\rho^-$	$K^-\pi^+$	21.9±5.2	0.71±0.17	0.74±0.10±0.14 ± 0.03
	$K^-\pi^+\pi^0$	39.8±7.2	1.08±0.20	
	$K^-\pi^+\pi^+\pi^-$	14.6±4.6	0.52±0.17	

The relative sign of a_1 and a_2 can be determined since, for the decays of the charged B mesons, both amplitudes contribute, with constructive or destructive interference depending on the sign of a_2/a_1. BSW found $a_2/a_1 \sim -0.22$ by extrapolating the QCD amplitudes from the scale $\mu = m_c$ to $\mu = m_b$ and assuming $\xi = 0$ as seemed to be needed for charm decays. This negative sign is quite clearly needed in D decays though with $\xi = 1/3$ ($N_C = 3$), the calculation for B decays can lead to a significant positive value.

CLEO determines the sign of a_2/a_1 in B decays by taking ratios of the four branching fractions given in Table 2 and the corresponding branching fractions for

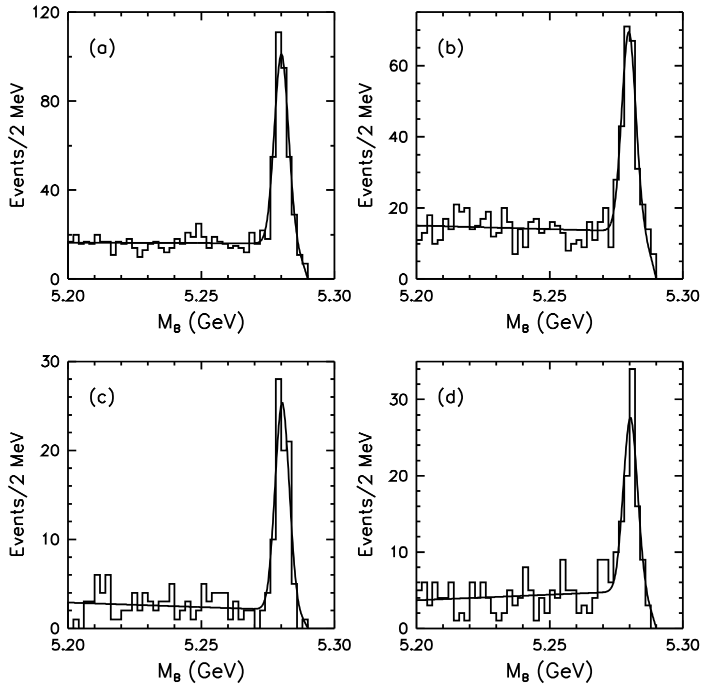

Fig. 1. CLEO II beam-constrained mass distributions for (a) $B^- \to D^0\pi^-$, (b) $B^- \to D^0\rho^-$, (c) $B^0 \to D^+\pi^-$, and (d) $B^0 \to D^+\rho^-$.

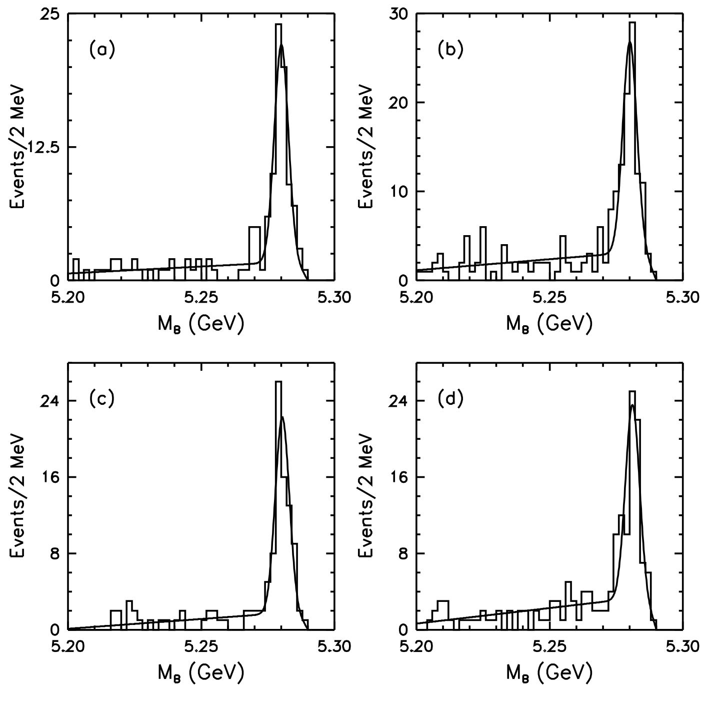

Fig. 2. CLEO II beam-constrained mass distributions for (a) $B^- \to D^{*0}\pi^-$, (b) $B^- \to D^{*0}\rho^-$, (c) $B^0 \to D^{*+}\pi^-$, and (d) $B^0 \to D^{*+}\rho^-$.

TABLE 2. Measured branching fractions for four B^- decay modes.

B^- Mode	D mode	# of events	$\mathcal{B}(\%)$	$\mathcal{B}$ average (%)
	$K^-\pi^+$	76.3 ± 9.1	0.48 ± 0.06	
$D^0\pi^-$	$K^-\pi^+\pi^0$	134 ± 15	0.62 ± 0.07	$0.55\pm0.04\pm0.05 \pm 0.02$
	$K^-\pi^+\pi^+\pi^-$	94 ± 11	0.57 ± 0.07	
	$K^-\pi^+$	80 ± 9	1.40 ± 0.18	
$D^0\rho^-$	$K^-\pi^+\pi^0$	42 ± 9	1.04 ± 0.23	$1.35\pm0.12\pm0.14 \pm 0.04$
	$K^-\pi^+\pi^+\pi^-$	90.4 ± 12.1	1.53 ± 0.20	
	$K^-\pi^+$	13.3 ± 3.8	0.36 ± 0.13	
$D^{*0}\pi^-$	$K^-\pi^+\pi^0$	37.7 ± 6.9	0.63 ± 0.12	$0.52\pm0.07\pm0.06 \pm 0.04$
	$K^-\pi^+\pi^+\pi^-$	20.0 ± 4.9	0.52 ± 0.13	
	$K^-\pi^+$	25.7 ± 5.4	1.74 ± 0.37	
$D^{*0}\rho^-$	$K^-\pi^+\pi^0$	43.8 ± 7.8	2.24 ± 0.40	$1.68\pm0.21\pm0.25 \pm 0.12$
	$K^-\pi^+\pi^+\pi^-$	16.9 ± 4.6	1.19 ± 0.35	

the B^- decays given in Table 1:

$$\begin{aligned}
R_1 &= \frac{\mathcal{B}(B^- \to D^0\pi^-)}{\mathcal{B}(\bar{B}^0 \to D^+\pi^-)} = (1 + 1.23a_2/a_1)^2 \\
R_2 &= \frac{\mathcal{B}(B^- \to D^0\rho^-)}{\mathcal{B}(\bar{B}^0 \to D^+\rho^-)} = (1 + 0.66a_2/a_1)^2 \\
R_3 &= \frac{\mathcal{B}(B^- \to D^{*0}\pi^-)}{\mathcal{B}(\bar{B}^0 \to D^{*+}\pi^-)} = (1 + 1.29a_2/a_1)^2 \\
R_4 &= \frac{\mathcal{B}(B^- \to D^{*0}\rho^-)}{\mathcal{B}(\bar{B}^0 \to D^{*+}\rho^-)} \approx (1 + 0.75a_2/a_1)^2.
\end{aligned} \tag{II.4}$$

From the measured ratios given in Table 3 and the BSW-model expectations given above, they find $a_2/a_1 = +0.23 \pm 0.04 \pm 0.04 \pm 0.10$. Also shown in the table are predictions of the model of Reader and Isgur (RI)[8] in which they take the values of a_1 and a_2 from the QCD calculations ($\xi = 1/3$) and use HQET to derive the needed form factors. This model gives consistently smaller values of the ratios than either the data or the BSW-model predictions. Unlike the situation in charm decays, the interference is clearly constructive in B decays; this can increase the branching fraction for some decays by more than a factor of three compared with the value for $a_2/a_1 < 0$.

TABLE 3. Ratios of branching fractions and predictions for both signs of a_2/a_1.

Ratio	$a_2/a_1 = -0.24$	$a_2/a_1 = 0.24$	CLEO II	RI model
R_1	0.50	1.68	$1.89 \pm 0.26 \pm 0.32$	$1.20 - 1.28$
R_2	0.71	1.34	$1.67 \pm 0.27 \pm 0.30$	$1.09 - 1.12$
R_3	0.48	1.72	$2.00 \pm 0.37 \pm 0.28$	$1.19 - 1.27$
R_4	0.41	1.85	$2.27 \pm 0.41 \pm 0.41$	$1.10 - 1.36$

The branching fractions given in Table 1 can also be used to test the factorization hypothesis which underlies all of the hadronic B decay theoretical predictions. By factorization we mean:

$$\Gamma\left(\bar{B}^0 \to D^{*+}h^-\right) = 6\pi^2 c_1^2 f_h^2 |V_{ud}|^2 \frac{d\Gamma}{dq^2}\left(\bar{B}^0 \to D^{*+}\ell^-\bar{\nu}_\ell\right)\Big|_{q^2=m_h^2}, \tag{II.5}$$

where c_1 is a small correction for hard-gluon radiation and f_h is the decay constant for multi-pion resonance h. The final term is taken from model-dependent fits to the $B^0 \to D^{*+}\ell^-\bar{\nu}_\ell$ data. In order to test factorization, one can find the ratio of the left- and right-hand sides of Eq. (II.5) for $h = \pi, \rho, a_1$. For the CLEO data the ratios for these three modes are 0.92 ± 0.19, 0.91 ± 0.19 and 1.33 ± 0.31, respectively. Since 1.0 is expected, the factorization hypothesis is validated at the $\sim 20\%$ level for q^2 up to about 1.2 GeV/c^2.

III. *B* semileptonic branching fraction

The measured B semileptonic branching fraction has been substantially lower than the theoretically expected value for several years. This has led to improvements in theoretical predictions[9),10)] as well as experimental refinements. Most experimental measurements find a value below 11%. Naive theoretical predictions give about 15%, which is reduced to $\sim$12.5% with perturbative and non-perturbative corrections.[10)] A recent paper[11)] suggests that the non-leptonic decay rate may be enhanced due to an anomalously large $b \to c\bar{c}s$ transition rate. However, until recent measurements, it has not been clear whether further refinements in the theoretical calculations are needed or the experimental measurements are systematically low.

The CLEO-II collaboration has used a sample of inclusive leptons to determine $\mathcal{B}(B \to X\ell\nu)$.[14)] They use muons above 1.3 GeV/c and electrons above 0.5 GeV/c, as shown in Fig. 3. Also shown in this figure is the fit to the ACCMM model[15] and the fit amounts of $b \to c\ell\nu$ and cascade semileptonic decays. The results are:

$$\begin{aligned} \mathcal{B}(B \to X\ell\nu) &= (10.65 \pm 0.05 \pm 0.33)\% \quad \text{(ACCMM model)} \\ &= (10.42 \pm 0.05 \pm 0.33)\% \quad \text{(ISGW model)} \\ &= (10.98 \pm 0.10 \pm 0.33)\% \quad \text{(modified ISGW model)}, \end{aligned} \tag{III.1}$$

where the last line has the fraction of 'X' which is D^{**} included in the fit. In the ISGW model,[16] 11% of the leptons are accompanied by a D^{**}, but the χ^2 for the fit with this value is poor. When this fraction is allowed to float, its fit value is $(21 \pm 2 \pm 8)\%$ with a much improved χ^2.

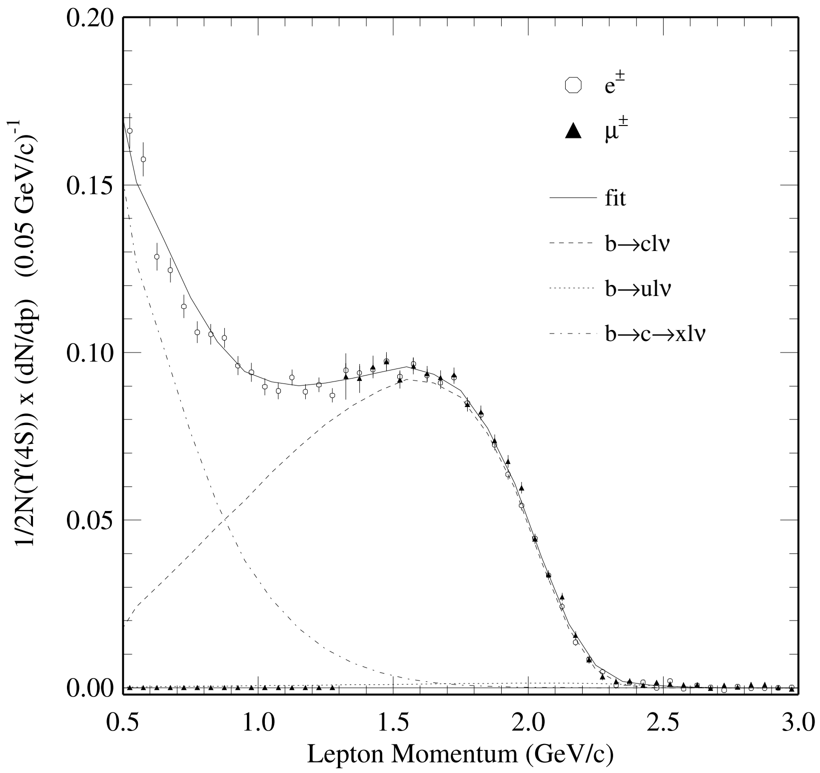

Fig. 3. The B semileptonic lepton spectra: electrons above 0.5 GeV/c are shown as open circles and muons above 1.3 GeV/c are shown as filled triangles. The best fit to the ACCMM model is shown as the solid line, with the $b \to c\ell\nu$ and cascade components indicated by the dashed and dot-dashed lines respectively.

The ARGUS collaboration has used an innovative approach which is less model dependent than the method described above and also is insensitive to possible non-$B\bar{B}$ decays of the $\Upsilon(4S)$ resonance, which could contribute in and above the signal region of the inclusive analysis. The idea is to tag events with a lepton of momentum greater than 1.4 GeV/c. This sample is nearly pure $b \to c\ell\nu$ decays. They then search for a second lepton in the event with the opposite charge from the tag (same-charge leptons will be dominantly from the $b \to c \to \ell$ cascade process). There are two possibilities for the opposite-sign lepton. In the signal process the lepton is from the $b \to c\ell\nu$ decay of the non-tag B, but there is a substantial background where the lepton is from a $c \to \ell$ decay, where c arises in the decay of the tag B. Since the leptons from the latter process tend to be quite anti-correlated in direction with the tag lepton, it is suppressed by requiring $\cos\theta_{\ell\ell} > 0$, where $\theta_{\ell\ell}$ is the angle between the two leptons. This cut reduces the cascade and continuum backgrounds by a factor of 7 and 4, respectively.

In Fig. 4(a) and (b), we show the momentum distributions for the $b \to c\ell\nu$ and $b \to c \to \ell$ data samples. Also shown are fits to the data for the ACCMM and ISGW models. It is evident that the effect of the models on the efficiency above 0.6 GeV/c is negligible. From this analysis ARGUS finds $\mathcal{B}(B \to X\ell\nu) = (9.6 \pm 0.5 \pm 0.4)\%$. A more recent analysis by the CLEO II collaboration using the same technique finds $\mathcal{B}(B \to X\ell\nu) = (10.50 \pm 0.28 \pm 0.37)\%$. All of these measurements are in good agreement, indicating that further theoretical work is likely to find even more enhancements to the B hadronic decay rate or that the semileptonic decay rate has been over-estimated.

IV. B semileptonic decays and V_{cb}

Several methods can be used to extract V_{cb} from B semileptonic decay rates. The three that I will describe here involve using the $B^0 \to D^{*+}\ell^-\nu_\ell$ or inclusive B-semileptonic branching fractions, or using the q^2 dependence of the decay $B^0 \to D^{*+}\ell^-\nu_\ell$ in conjunction with the predictions of HQET.

In the first approach, the CLEO-II collaboration has measured[17] $\mathcal{B}(B^0 \to D^{*+}\ell^-\nu_\ell) = 0.0450 \pm 0.0044 \pm 0.0044$. Using model dependent form factors and a value of $\tau_B = 1.49 \pm 0.03$ ps, they find $V_{cb} = 0.038 - 0.044$ for a range of models.

In the second method the CLEO-II collaboration uses the inclusive B-semileptonic branching fraction measurement discussed in the previous chapter to determine V_{cb}. Using the same B lifetime as above, they find for both the ACCMM and ISGW models, $V_{cb} = 0.042 \pm 0.001 \pm 0.004$.

Finally, there is the HQET method which until recently was expected to be the method of choice due to claims of little model dependence.[18),19)] Some recent work[20)] disagrees with the previous calculations so there is $\sim$10% uncertainty in this method at present. The method involves use of the Lorentz-invariant quantity

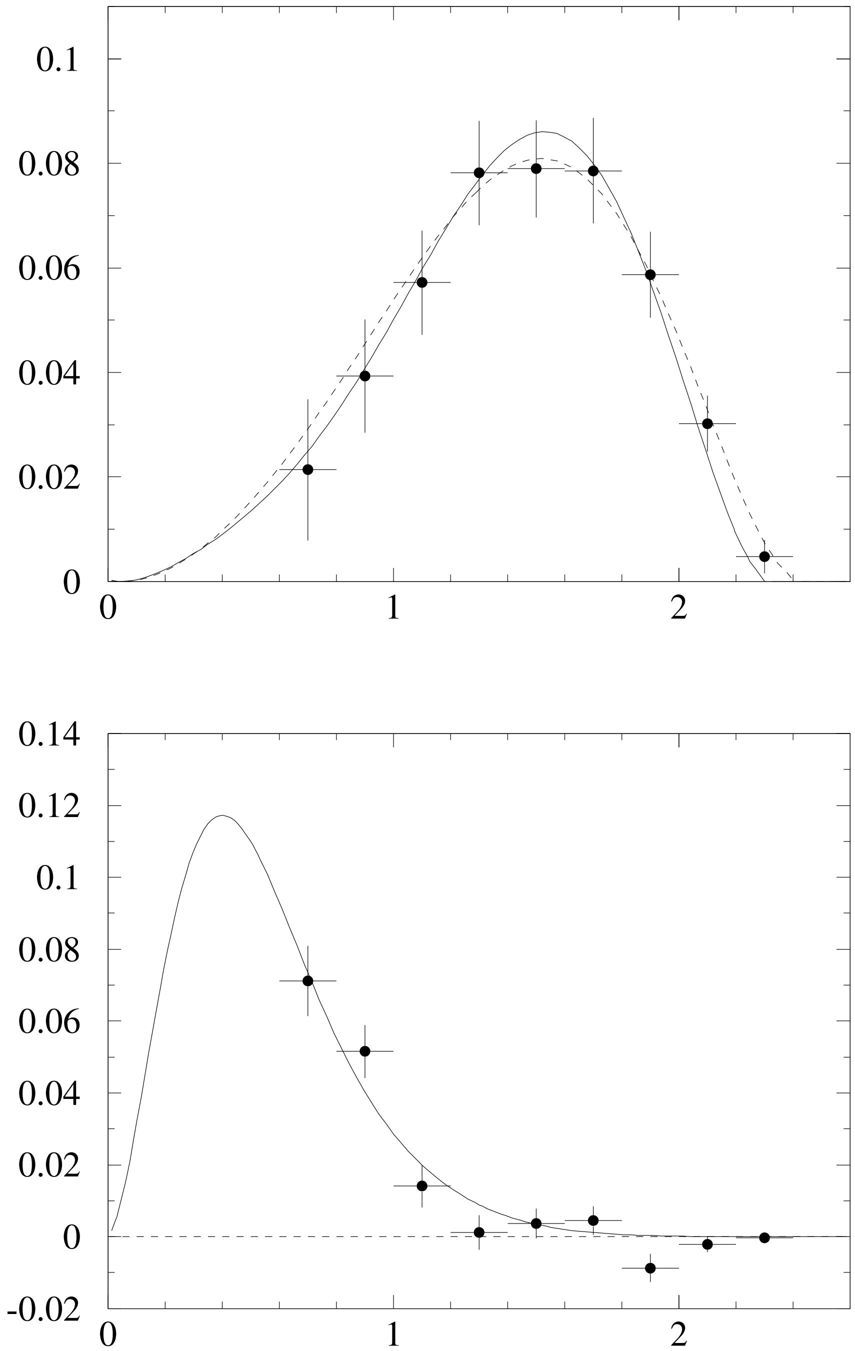

Fig. 4. Plots of the momentum distributions for the double-lepton-tag ARGUS analysis for (a) events from the signal process $b \to c\ell\nu$, and (b) $b \to c \to \ell$ cascade events. Fits to the predicted shape for the ACCMM and ISGW models are shown by solid and dashed lines, respectively.

$y \equiv v_B \cdot v_{D^*}$, where we have assumed the decay $B \to D^* \ell \nu$ though the decay $B \to D \ell \nu$ can also be used. Given that the B is nearly at rest, y can be written

$$y = \frac{m_B^2 + m_{D^*}^2 - q^2}{2 m_B m_{D^*}}.$$

The HQET prediction for the distribution $d\Gamma/dy$ is that it is proportional to V_{cb}^2 and to the square of the "Isgur-Wise" function $\xi(y)$. Neubert[19)] finds $\xi(1) = 0.97 \pm 0.04$; it is this prediction which has recently been challenged by Shifman *et al.*,[20)] who find $\xi(1) = 0.89 \pm 0.03$, though another recent calculation[21)] is in good agreement with Neubert.

The distribution $d\Gamma/dy$ has been measured by the CLEO-II collaboration and is shown in Fig. 5. By extrapolating to $y = 1$ and using $\xi(1) = 0.97 \pm 0.04$, they find V_{cb} to be in the range 0.037 to 0.038, depending on the shape used for $\xi(y)$, with statistical and systematic uncertainties of 0.006 and 0.004, respectively. The value of V_{cb} would increase by 8% if the value from Shifman *et al.* were used.

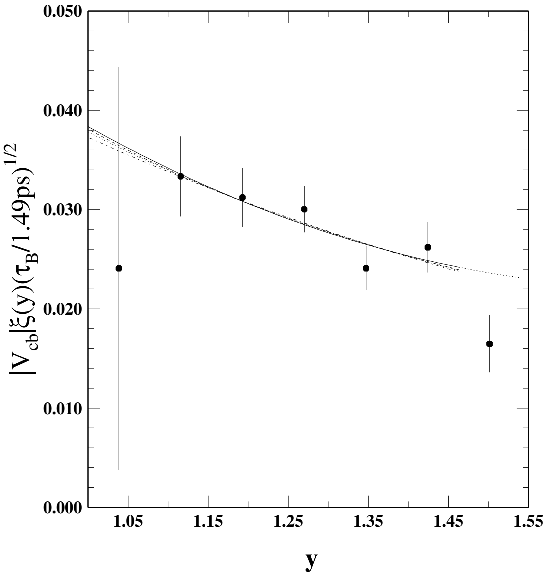

Fig. 5. The efficiency corrected $d\Gamma/dy$ distribution for CLEO $B^0 \to D^{*+} \ell^- \nu$ events. The curves are for four functional forms for $\xi(y)$.

All of these measurements of V_{cb} are consistent with a value near 0.040. A recent review by Stone[22)] uses the above measurements and older measurements by CLEO I and ARGUS to determine $V_{cb} = .038 \pm 0.003$, where the error is dominated by the range of model predictions.

A new measurement of $d\Gamma/dy$ and V_{cb} by the CLEO-II collaboration has recently been submitted for publication.[23] This result accounts for the motion of the B in smearing y and performs a likelihood fit to the data. Both the decays $B^0 \to D^{*+}\ell^-\nu_\ell$ and $B^- \to D^{*0}\ell^-\nu_\ell$ are used. Assuming $\xi(1) = 0.97 \pm 0.04$, they find $V_{cb} = 0.0355 \pm 0.0019 \pm 0.0020 \pm 0.0014$, where the final systematic error is due to the uncertainty in $\xi(1)$. This value is somewhat lower than the values given above, though consistent with them.

V. The end point of the B semileptonic spectrum and V_{ub}

Even though $b \to u\ell\nu$ decays comprise only about 1% of the semileptonic decay rate, it is possible to isolate such decays since they populate the region beyond the end point of the $b \to c\ell\nu$ spectrum due to the lighter mass of the u quark. The existence of these decays was established a few years ago by CLEO[24] and confirmed by ARGUS.[25] A recent result from the CLEO II collaboration[26] has re-confirmed the existence of these decays though at a substantially smaller level.

The new CLEO-II analysis uses much tighter cuts than the previous CLEO analysis to reduce backgrounds from continuum $q\bar{q}$ events. The efficiency is reduced by about a factor of two in the process. In Fig. 6(a), a 7σ excess can be seen in the signal region, 2.3-2.6 GeV/c. An analysis similar to the previous ones with looser cuts is shown in Fig. 6(b). There are more than twice as many signal events but also about ten times as much continuum background. Since only a small fraction of all $b \to u\ell\nu$ decays fall in the signal region, the correction to extract the full decay rate (and hence V_{ub}) is quite sensitive to the modelling of the spectrum near the end point. In Table 4, we show the results for four theoretical models. The situation can be summarized approximately by $V_{ub} = 0.08 \pm 0.02$, where the error is totally dominated by the disagreement between the models.

TABLE 4. $|V_{ub}/V_{cb}|$ for four theoretical models applied to the CLEO-II data.

Model	$\lvert V_{ub}/V_{cb}\rvert$
ISGW[16]	0.101 ± 0.010
KS [12]	0.056 ± 0.006
WSB [13]	0.073 ± 0.007
ACCMM[15]	0.076 ± 0.008

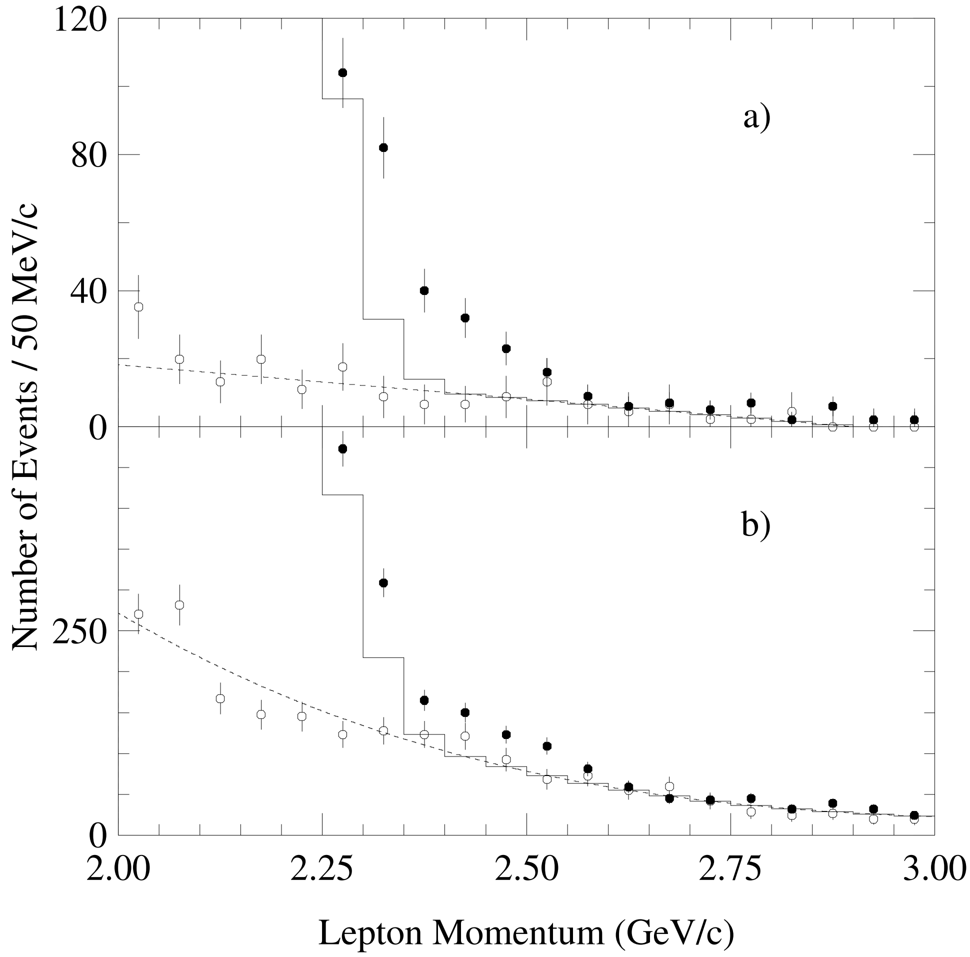

Fig. 6. CLEO-II lepton momentum spectra for on-resonance data (filled circles) and scaled off-resonance data (open circles) for (a) tight-cut analysis; (b) loose-cut analysis. The dashed line is a fit to the off-resonance data and the solid line is the background prediction from the off-resonance data and the expected $b \to c\ell\nu$ component.

VI. Rare B decays: penguins and V_{ub}

Until recently the most interesting rare B decays, with expected branching fractions of $\sim 10^{-5}$, have been inaccessible since samples of more than a million B's are needed to be sensitive to such small branching fractions. The situation is beginning to change with the large samples accumulated by LEP and CLEO. We will describe an ARGUS search for evidence for the decay $b \to s$ gluon, the CLEO-II observations of signals for $B \to K^*\gamma$ and $B^0 \to K^+\pi^-/B^0 \to \pi^+\pi^-$ and new searches from CLEO for other rare decays.

A. Inclusive search for b $\rightarrow$ s gluon using tagging

In the Standard Model, the one-loop process $b \rightarrow s$ gluon is expected to occur with a branching fraction of about 2%.[27] This value could be increased to as much as 20% in models with charged-Higgs bosons. Such large values would be of considerable significance since an enhancement of the hadronic decay rate could account for the relatively small semileptonic branching fraction discussed in chapter III.

The ARGUS collaboration has searched for such decays by using a "tagging" technique whereby the other B in the event is detected. They tag this B via the decays: $B \rightarrow D^{(*)}\ell^-\nu$, $B \rightarrow D^{(*)}\pi^-$, $B \rightarrow D^{(*)}\rho^-$ and $B \rightarrow D^{(*)}a_1^-$, with $D^* \rightarrow D\pi$ or $D^* \rightarrow D\gamma$ and $D^0 \rightarrow K^-\pi^+(\pi^0)$, $D^0 \rightarrow K^-\pi^+\pi^+\pi^-$, $D^0 \rightarrow K_S\pi^+\pi^-(\pi^0)$, $D^+ \rightarrow K^-\pi^+\pi^+(\pi^0)$ or $D^+ \rightarrow K_S\pi^+(\pi^0)$. The overall tagging efficiency is 0.9%, dominated by the semileptonic-decay tag (the lepton is required to have a momentum above 1.4 GeV/c).

For tagged events, ARGUS looks for a $b \rightarrow s$ gluon signal by considering decays with a kaon and from one to seven charged pions, where the kaon can be either charged or neutral. The invariant mass distribution of such signal candidates is shown in Fig. 7. There is one entry per event, selected according to the best total energy when the kaon identification is ambiguous. Clearly the continuum background is small; they estimate 0.07 ± 0.03 events by relaxing the energy cut from two to 40 standard deviations. Of the seven events in the B-mass region of Fig. 7, five are consistent with coming from $b \rightarrow c$ transitions, with either D's or ψ's in the final state. The remaining two events, shown hatched in the figure, are inconsistent with D, D_S, ψ, η_c and χ_c hypotheses at a level of at least 4σ. These events are also kinematically inconsistent with B decays to baryons.

The two candidate events are interpreted as decays $B^0 \rightarrow K^+\pi^-$ and $B^- \rightarrow K^-\pi^-\pi^-\pi^+\pi^+$, though without conclusive kaon identification, the $b \rightarrow u$ interpretation of these decays cannot be excluded. However, the efficiency for $b \rightarrow u$ decays is about a factor of four below the 2% estimate for the $b \rightarrow s$ gluon signal. From the two events observed, they find $\mathcal{B}(b \rightarrow s \text{ gluon}) = 0.026^{+0.017}_{-0.015}$. No systematic errors have been assigned since the substantial model dependence is still being evaluated. This preliminary result is in good agreement with the expectation for a $b \rightarrow s$ gluon signal.

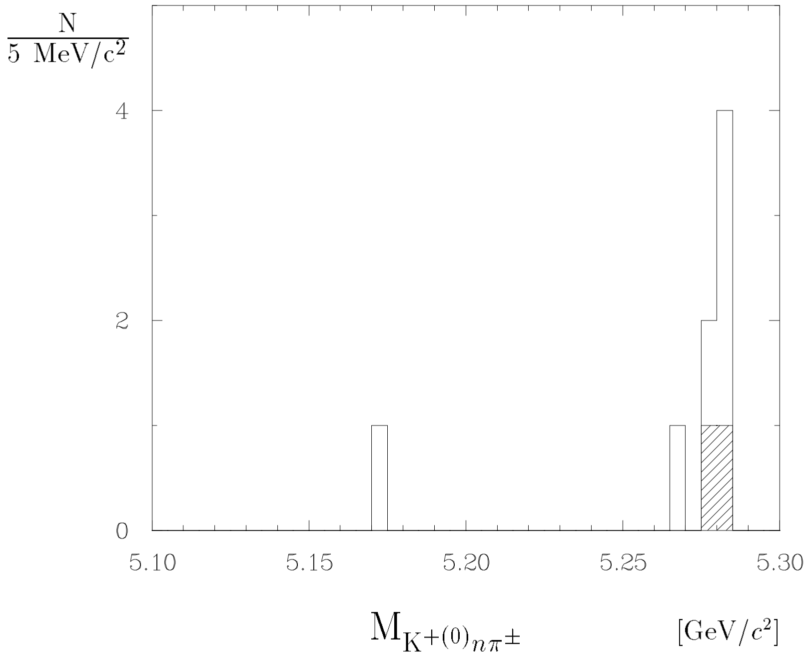

Fig. 7. The invariant mass distribution for the tagged events in the ARGUS $b \to s$ gluon search. Unshaded events are consistent with a $b \to c$ hypothesis and the hatched events are not.

B. The decays $\mathbf{B^0} \to \pi^+\pi^-$ and $\mathbf{B} \to \mathbf{K}^+\pi^-$

The decays $B^0 \to \pi^+\pi^-$ and $B^0 \to K^+\pi^-$ are of considerable interest since the former is presumed to be dominated by $b \to u$ transitions and the latter is expected to proceed dominantly via so-called gluonic "penguin" diagrams. These diagrams are shown in Fig. 8 along with the suppressed versions which contribute to the other mode. Both of these decays are interesting for CP violation, $B^0 \to \pi^+\pi^-$ because the final state is a CP eigenstate and could be used to measure the angle α of the unitarity triangle, and $B^0 \to K^+\pi^-$ because similar final states also may be used to measure CP violation angles and the penguin amplitudes are expected to complicate the analysis of $B^0 \to \pi^+\pi^-$.

The CLEO II collaboration has reported[28)] a signal for these modes, though due to limited statistics, they only claim a signal in the sum of the two modes. They perform a maximum likelihood fit using dE/dx information for each track, the total energy of the candidate, the "beam-constrained" mass for the candidate ($m_{\rm BC} = \sqrt{E_{\rm beam}^2 - p^2}$), and a shape variable used to reject continuum $q\bar{q}$ background. The results of the fit are shown in the contour plot of Fig. 9. The individual $\pi\pi$ and

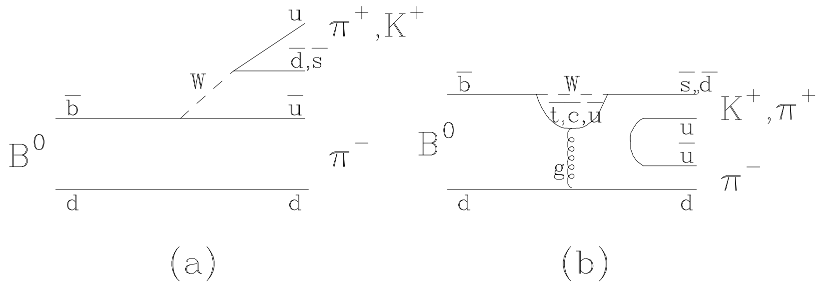

Fig. 8. (a) Spectator diagrams for $B^0 \to \pi^+\pi^-$ and $B^0 \to K^+\pi^-$ and (b) penguin diagram for the same modes.

$K\pi$ signals have significance of only 2.5 and 2.8 standard deviations, respectively. However, the summed signal is 5.4σ from zero, 4.2σ after conservatively accounting for all systematic errors. A summary of the fit results and the derived branching fractions and limits are given in Table 5. These results are in agreement with the theoretical predictions of $1.8 \pm 0.8 \times 10^{-5}$ for $B^0 \to \pi^+\pi^-$ [5] and $1 - 2 \times 10^{-5}$ for $B^0 \to K^+\pi^-$.[29]

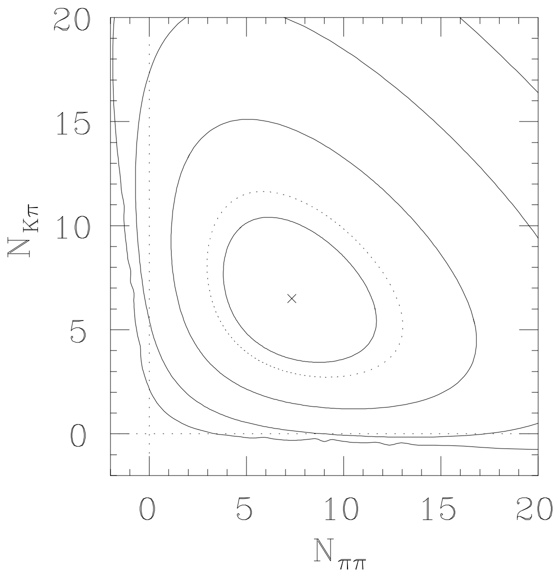

Fig. 9. Likelihood contours for the CLEO-II $B^0 \to \pi^+\pi^-$ and $B^0 \to K^+\pi^-$ analysis. The solid lines are $1 - 4\sigma$ contours and the dotted line is the 1.28σ contour.

TABLE 5. Measured branching fractions and 90% CL upper limits (UL).

Mode	$N_{\rm fit}$	B (10^{-5})	UL (10^{-5})
$\pi^+\pi^-$	$7.2^{+4.3}_{-3.5}$	$1.3^{+0.8}_{-0.6} \pm 0.2$	2.9
$K^+\pi^-$	$6.4^{+3.9}_{-3.1}$	$1.1^{+0.7}_{-0.6} \pm 0.2$	2.6
K^+K^-	$0.0^{+0.8}_{-0.0}$	$0.0^{+0.2}_{-0.0}$	0.7
$\pi^+\pi^-$ or $K^+\pi^-$	$13.6^{+4.7}_{-3.9}$	$2.4^{+0.8}_{-0.7} \pm 0.2$	

C. The decays $\mathbf{B \to K\phi}$, $\mathbf{B \to K^*\phi}$ and $\mathbf{B \to \phi\phi}$

The decays $B \to K\phi$, $B \to K^*\phi$ are very interesting since they proceed via penguin diagrams as indicated in Fig. 10. The decays of the charged B's also can occur via an annihilation diagram, though this should be negligible. The decay $B \to \phi\phi$ is expected to be very small since it occurs only through box and loop diagrams with two W/Z's or via a OZI-suppressed loop diagram.

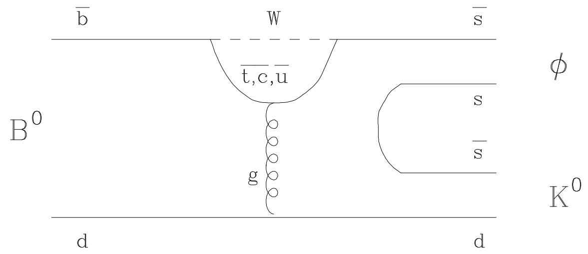

Fig. 10. The penguin diagram which is expected to dominate all ϕ decays modes discussed in the text.

The CLEO-II collaboration has searched for these modes[31] using a technique similar to the $B^0 \to \pi^+\pi^-$ analysis but without the likelihood fit. A signal region is defined such that candidates have a total energy within 60 MeV (2.5-4σ depending on mode) of the beam energy and a beam-constrained mass within 8 MeV/c^2 ($\sim 3\sigma$) of the B mass. A summary of the results is shown in Table 6. For the K^* modes, the decay going to a charged K is given, with the decay involving K_S in parentheses, since the former gives the more restrictive upper limit. Backgrounds are estimated from data taken just below the energy of the $\Upsilon(4S)$ resonance. Upper limits are found with the PDG prescription for limits in the presence of background; where the background is negligible, it is ignored in finding limits. In the case of the $K^+\phi$ and $K^{*0}\phi$ final states, the limits given in the table are getting close to the theoretical predictions.[29),30]

TABLE 6. CLEO III results for B decays with ϕ's.

Mode	Signal events	Estimated background	$\mathcal{B}$ limit 90% CL	Theoretical range [29,30]
$\mathcal{B}(B^+ \to K^+\phi)$	2	3.0	2.1×10^{-5}	$0.6 - 1.4 \times 10^{-5}$
$\mathcal{B}(B^+ \to K^{*+}(892)\phi)$	1(1)	2.0(0.1)	1.2×10^{-4}	$0.2 - 3.1 \times 10^{-5}$
$\mathcal{B}(B^0 \to K^0\phi)$	1	0.2	1.2×10^{-4}	$0.7 - 1.1 \times 10^{-5}$
$\mathcal{B}(B^0 \to K^{*0}(892)\phi)$	5(0)	3.6(0.1)	6.0×10^{-5}	$0.2 - 3.1 \times 10^{-5}$
$\mathcal{B}(B^0 \to \phi\phi)$	0	0.1	4.1×10^{-5}	

D. B decays to two leptons

B decays to a pair of leptons are expected to be quite rare,[32] partly since they occur only via higher-order diagrams such as those shown in Fig. 11, and partly since they are helicity suppressed. In the Standard Model, only the decay to a pair of taus has a significant branching fraction ($\sim 10^{-8}$), and it is extremely difficult to detect this mode with high efficiency. Nevertheless searches for di-lepton modes are of interest since models with charged Higgs[33] or leptoquarks[34] could have observable rates.

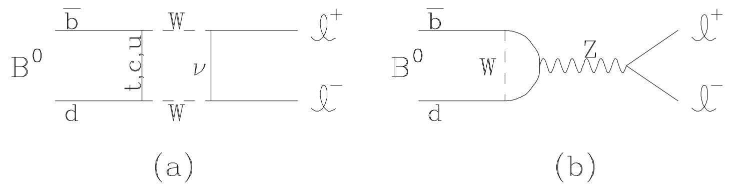

Fig. 11. The primary diagrams for the decays $B \to ee$ and $B \to \mu\mu$: (a) box diagram and (b) loop diagram.

The CLEO-II collaboration has searched for the final states ee, $\mu\mu$, $e\mu$, $e\tau$ and $\mu\tau$. The study of the modes without taus is similar to the $B^0 \to \pi^+\pi^-$ analysis (without the likelihood fit) with the addition of lepton identification. The search for the decay modes with taus involves looking for pions with momentum above 1.75 GeV/c; such pions originate mostly from the decay $\tau \to \pi\nu_\tau$ and to a lesser extent from the decay $\tau \to \rho\nu_\tau$. In addition a lepton of momentum between 2.2 and 2.5 GeV/c is required and the combined energy of the pion, lepton and neutrino is required to be within 300 MeV of the B mass. The neutrino momentum is taken to be the total momentum of the pion and lepton since the B is nearly at rest.

In Table 7, we summarize the results of this search, with the branching fraction upper limits derived as in the previous section. These measurements improve upon previous limits by about a factor of 5 in the ee and $e\mu$ modes and are the first measurements of the $e\tau$ and $\mu\tau$ modes. While these results are not approaching Standard Model sensitivity, they do place some constraints on some extensions of the Standard Model.

TABLE 7. Results from CLEO II for di-lepton decays of the B.

Mode	N_{obs}	$N_{\rm UL}$	Upper limit (90% CL)	SM Theory [32]
$B^0 \to e^+e^-$	0	2.3	5.9×10^{-6}	2×10^{-15}
$B^0 \to \mu^+\mu^-$	0	2.3	5.9×10^{-6}	8×10^{-11}
$B^0 \to e^\pm\mu^\mp$	0	2.3	5.9×10^{-6}	0
$B^0 \to e^\pm\tau^\mp$	4	8.0	5.3×10^{-4}	0
$B^0 \to \mu^\pm\tau^\mp$	6	10.5	8.3×10^{-4}	0

E. Electromagnetic penguin decays: $\mathbf{B \to K^*\gamma}$ and inclusive $\mathbf{b \to s\gamma}$

Among the most interesting of all rare-B decays are the electromagnetic penguin decays involving the transition $b \to s\gamma$. Now that the mass of the top quark is known[37)] to be $174 \pm 10 \pm 13$ GeV/c^2, the range of branching fraction predictions for the inclusive decay $b \to s\gamma$ has narrowed somewhat to within about 25% of $\sim 3 \times 10^{-4}$. This $\sim$25% range is due primarily to the uncertainty in the relevant QCD mass scale;[35),36)] the QCD corrections are about a factor of 4 and the present state of the art is only a "leading-log" QCD calculation. Once the higher order "next-to-leading-log" calculation is performed (involving up to three-loop diagrams!), the QCD scale dependence should be reduced to below 5%.[36)] This would provide fairly precise measurements of V_{ts}, or sensitivity to non-Standard-Model physics if one assumes $|V_{ts}| = |V_{cb}|$ as expected from unitarity of the CKM matrix.

The CLEO-II collaboration has searched for both the inclusive and exclusive decays. The inclusive search is difficult due to the presence of continuum $q\bar{q}$ background. A variety of cuts are employed to reject continuum events but there remains a background of 566 ± 35 events in the signal region, $2.2 < E_\gamma < 2.7$ GeV, estimated from off-resonance data. There are 635 events in the signal region of the on-resonance data, resulting in a net yield of 69 ± 43 events. Since this signal is not significant they calculate a 95% confidence level upper limit, $\mathcal{B}(b \to s\gamma) < 5.4 \times 10^{-4}$, not far above the expected value. Though this limit does not quite eliminate all charged-Higgs models, it severely restricts the parameter space for such models.[38]

While the inclusive decay can be simply calculated, the fragmentation process is difficult to model and there is a wide range of predictions[39] for the fraction of the inclusive rate which appears in the $K^*(892)\gamma$ final state. Recent predictions mostly fall in the range 6-20%. A representative diagram for this process is shown in Fig. 12.

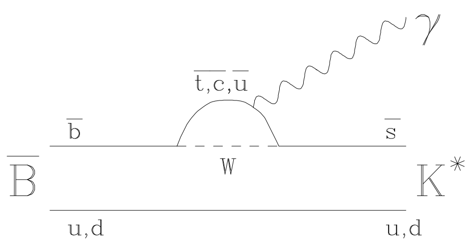

Fig. 12. A diagram for the decay $B \to K^*\gamma$. The photon can be radiated from any of the four upper lines.

The CLEO-II collaboration has reported[40] a signal for this decay with events in both the $B \to K^{*0}\gamma$ and $B^- \to K^{*-}\gamma$ decay modes. They search for the latter mode in both the $K_S\pi^-$ and $K^-\pi^0$ decays of the K^*. After making a variety of cuts to suppress continuum background, the $K^*\gamma$ signal is required to have an invariant mass within 6 MeV/c^2 of the B mass and an energy within 90 MeV of the beam energy. In Fig. 13, we show the mass distribution of events passing all cuts except the mass cut; there is a clear signal of 13 events of which two are expected to be background. Backgrounds are reliably estimated from the data using off-resonance data and mass and energy sideband regions. Table 8 summarizes the results of the analysis. If the two decay modes are assumed to have equal branching fractions, they find an average $\mathcal{B}(B \to K^*\gamma) = (4.5 \pm 1.5 \pm 1.9) \times 10^{-5}$. This result is quite consistent with expectations from the predicted inclusive rate and the fraction going to $K^*\gamma$ given above.

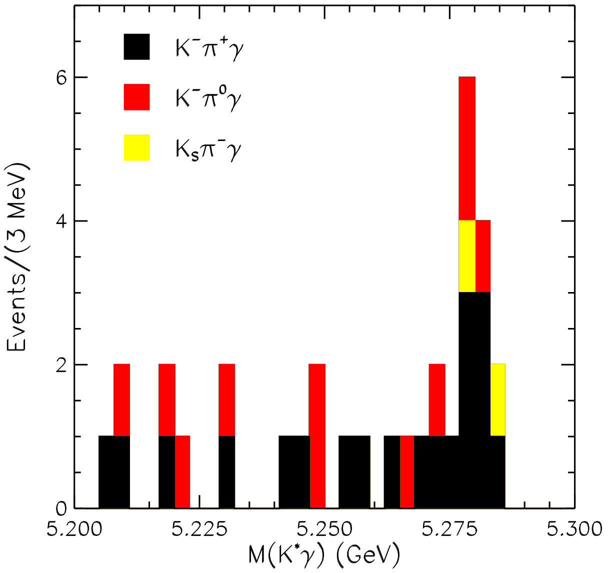

Fig. 13. The CLEO-II $K^*\gamma$ mass distribution for $B \to K^{*0}\gamma$ and $B^- \to K^{*-}\gamma$ candidates.

TABLE 8. Results from CLEO II for the decay $B \to K^*\gamma$.

	$B^0 \to K^{*0}\gamma$	$B^- \to K^{*-}\gamma$	
	$K^{*0} \to K^+\pi^-$	$K^{*-} \to K^0_S\pi^-$	$K^{*-} \to K^-\pi^0$
Signal Events	8	2	3
Sideband Events	41	2	10
Sideband Scale Factor	37.6	40	12
Sideband Background	1.1±0.2	0.05±0.03	0.8±0.3
Binomial Probability	3.5×10^{-5}	3.7×10^{-3}	7.3×10^{-2}
Residual $B\overline{B}$ Background	0.30±0.15	0.01±0.01	0.10±0.05
Efficiency	(11.9±1.8)%	(2.0±0.3)%	(3.1±0.5)%
Branching Ratio	$(4.0\pm1.7\pm0.8)\times10^{-5}$	$(5.7\pm3.1\pm1.1)\times10^{-5}$	

VII. Conclusions

CLEO measurements of the decays $B \to D\pi$ and $B \to D\rho$ have been used to test the factorization hypothesis and the BSW model of hadronic B decays. CLEO semileptonic B-decay data have been used to measure V_{cb} and V_{ub} with improved accuracy. A novel tagging approach from ARGUS along with precise results from CLEO confirm that the B semileptonic branching fraction is less than 11%. A new search by ARGUS finds evidence for inclusive $b \to s$ gluon decays and presents a preliminary measurement of the branching fraction for this process. CLEO has searched for several rare B decays, with signals observed for $B \to K^*\gamma$ and the sum of $B^0 \to K^+\pi^-$ and $B^0 \to \pi^+\pi^-$. The sensitivity in some channels such as $B^+ \to K^+\phi$ is approaching the theoretical predictions. Finally, a limit from CLEO on the inclusive process $b \to s\gamma$ severely constrains extensions of the Standard Model such as those involving charged Higgs.

REFERENCES

1. N. Cabibbo, ***Phys. Rev. Lett.*** **10** (1963) 531; M. Kobayashi and T. Maskawa, ***Prog. Theor. Phys.*** **49** (1973) 652.
2. M. Bauer, B. Stech, and M. Wirbel, ***Zeits. Phys. C*** **34** (1987) 103.
3. N. Isgur and M. B. Wise, ***Phys. Letters*** **B232** (1989) 113; *ibid.* **B237** (1990) 527.
4. See for example the discussion in M. Neubert, V. Rieckert, Q. P. Xu and B. Stech in ***Heavy Flavours***, edited by A. J. Buras and H. Lindner (World Scientific, Singapore, 1992).
5. A. Deandrea, N. Di Bartolomeo, R. Gatto and G. Nardulli, ***Phys. Letters*** **B318** (1993) 549.
6. M. S. Alam *et al.*, CLNS 94/1270, submitted to ***Phys. Rev. D.***
7. This and other recent CLEO results quoted here use the latest CLEO measurement of $\mathcal{B}(D^0 \to K^-\pi^+) = 0.0391 \pm 0.0008 \pm 0.0017$, the Mark III measurement $\mathcal{B}(D^+ \to K^-\pi^+\pi^+) = 0.091 \pm 0.014$ and PDG numbers for the ratio of other D decay modes to $\mathcal{B}(D^0 \to K^-\pi^+)$. The precise CLEO branching fraction measurements for D^* decays are also used.
8. C. Reader and N. Isgur, ***Phys. Rev. D*** **47** (1993) 1007.
9. G. Altarelli and S. Petrarca, ***Phys. Letters*** **B261** (1991) 303.
10. I. Bigi, B. Blok, M. A. Shifman and A. Vainshtein, ***Phys. Letters*** **B323** (1994) 408.
11. A. F. Falk, M. B. Wise and I. Dunietz, CALT-68-1933 (1994).
12. J. Körner and G. Schuler, ***Zeits. Phys. C*** **38** (1988) 511; *ibid.* **41** (1988) 690.
13. M. Wirbel, B. Stech and M. Bauer, ***Zeits. Phys. C*** **29** (1987) 637.
14. "Inclusive Measurement of B-meson Semileptonic Branching Fractions", J. Bartelt *et al.* contributed to the XVI International Symposium on Lepton-Photon Interactions, Ithaca, NY (1993), CLEO-CONF 93-19.

15. G. Altarelli, N. Cabibbo, G. Corbo, L. Maiani and G. Martinelli, ***Nucl. Phys.*** **B208** (1982) 365.
16. N. Isgur, D. Scora, B. Grinstein and M. Wise, ***Phys. Rev. D*** **39** (1989) 799.
17. "A Measurement of $\mathcal{B}(B^0 \to D^{*+}\ell^-\nu)$", G. Crawford *et al.* contributed to the XVI International Symposium on Lepton-Photon Interactions, Ithaca, NY (1993), CLEO-CONF 93-30.
18. M. Luke, ***Phys. Letters*** **B252** (1990) 447.
19. M. Neubert, ***Phys. Letters*** **B264** (1991) 455; M. Neubert, SLAC-PUB-6263 (to appear in Physics Reports).
20. M. Shifman, N. G. Ultrasev and A. Vainshtein, TPI-MINN-94/13-T.
21. T. Mannel, CERN-TH-7162-94.
22. S. Stone, HEPSY 93-11, to appear in ***B Decays***, $2^{\rm nd}$ edition, ed. by S. Stone, (World Scientific, Singapore, 1994).
23. "Measurement of the $B \to D^*\ell\nu$ Branching Fractions and V_{cb}", B. Barish *et al.* (submitted to ***Phys. Rev. D***, CLNS 94/1285.
24. R. Fulton *et al.*, ***Phys. Rev. Lett.*** **64** (1990) 16.
25. H. Albrecht *et al.*, ***Phys. Letters*** **B234** (1990) 409; *ibid.* **B255** (1991) 297.
26. J. Bartelt *et al.*, ***Phys. Rev. Lett.*** **71** (1993) 4111.
27. W-S. Hou, A. Soni and H. Steger, ***Phys. Rev. Lett.*** **59** (1987) 1521; R. Grigjanis, P. J. O'Donnell, M. Sutherland and H. Navelet,, ***Phys. Letters*** **B224** (1989) 209.
28. M. Battle *et al.*, ***Phys. Rev. Lett.*** **71** (1993) 3922-3926.
29. N. G. Deshpande and J. Trampetic, ***Phys. Rev. D*** **41** (1990) 895; L-L. Chau, H-Y. Cheng, W. K. Sze, H. Yao and B. Tseng, ***Phys. Rev. D*** **43** (1991) 2176; A. Deandrea, N. Di Bartolomeo, R. Gatto, F. Feruglio and G. Nardulli, ***Phys. Letters*** **B320** (1994) 170.
30. N. G. Deshpande and X-G. He, OITS-538 (1994).
31. "Search for the Exclusive Charmless Decays $B \to \phi X_s$, with $X_s = K^+,\ K_S,\ K^{*+},\ K^{*0}$ or ϕ", R. Ammar *et al.* contributed to the XVI International Symposium on Lepton-Photon Interactions, Ithaca, NY (1993), CLEO-CONF 93-23.
32. A. Ali, C. Greub, and T. Mannel, DESY Report 93-016.
33. J. L. Hewett, S. Nandi and T. G. Rizzo, ***Phys. Rev. D*** **39** (1993) 250; M. Sher and Y. Yuan, ***Phys. Rev. D*** **44** (1991) 461.
34. W. Buchmüller and D. Wyler, ***Phys. Letters*** **B177** (1986) 377; S. Davidson, D. Bailey, and B. A. Campbell, ***Zeits. Phys. C*** **61** (1994) 613.

35. A. Ali and C. Greub, ***Zeits. Phys. C*** **49** (1991) 431.
36. A. J. Buras, M. Misiak, M. Münz and S. Pokorski, MPI-Ph/93-77.
37. F. Abe *et al.* Fermilab-PUB-94-116-E (submitted to ***Phys. Rev. D***).
38. See for example V. Barger, M. Berger and R. J. Phillips, ***Phys. Rev. Lett.*** **70** (1993) 1368; J. Hewett, ***Phys. Rev. Lett.*** **70** (1993) 1045.
39. See C. Bernard, P. Hsieh and A. Soni, ***Phys. Rev. Lett.*** **72** (1994) 1402 and references therein.
40. R. Ammar *et al.*, ***Phys. Rev. Lett.*** **71** (1993) 674.